Journal of Solar Energy Research (JSER)

Journal homepage: www.jser.ut.ac.ir

Short Term Forecasting of Solar Irradiance Using Ensemble CNN-Bi-LSTM-MLP Model Combined with Error Minimization and CEEMDAN Pre-Processing Technique

Rijul Kumar Srivastava[a,*], Anuj Gupta[b]

[a]*Department of Mechatronics Engineering, Chandigarh University, Mohali, India.*
[b]*Department of Electronics and Communication Engineering, Chandigarh University, Mohali, India.*

ARTICLE INFO

Article Type:

Research Article

Received:08.12.2023
Accepted:22.05.2024

Keywords:
Solar irradiation
Preprocessing technique
Evaluation metrics
Forecasting
Error minimization

A B S T R A C T

Solar energy forecasting is necessary due to its variable and fluctuating nature, but it is also a challenge to predict accurately behaviour of solar irradiation. To capture this, the proposed methodology uses an ensemble model combined with error minimization and CEEMDAN Pre-processing technique. In this paper, data of two locations are used to predict short term forecasting of solar irradiation using seven developed models based on the proposed procedure. The use of hourly forecasting, CEEMDAN method, error minimization and ensemble hybrid model enhance the anti-interference capability of all developed model. Four-year data of New Delhi and Ahmedabad is used and sourced from NSRDB website. Out of all the proposed models CEEMDAN-CNN-BiLSTM-MLP with CEEMDAN_IMF_18 configured signal processing approach achieved least average RMSE, n-RMSE and MAE of both locations with values 13.215 W/m^2, 7.13% and 8.605 W/m^2 respectively and have maximum average R^2 (99.205%). When compared to persistence model, proposed model with this configuration was able to outperform with average percentage improvement 87.63%, 86.78%, 87.17% and 17.875% in terms of P_{RMSE}, P_{nRMSE}, P_{MAE} and P_{R^2} respectively. The proposed model outperforms existing techniques for solar irradiation forecasting, demonstrating greater efficiency and reliability, making it a valuable reference for future performance optimization.

1. Introduction

Solar energy is most utilized renewable energy source due to the ease of harvesting energy using solar grid of photovoltaic cells. These grids became more efficient since the monocrystalline bifacial solar panel came into market. Also, as the production of such panels increases leads to lower cost and in the

*Corresponding Author Email: rijulsrivastava@gmail.com

Cite this article: Srivastava, R., & Gupta, A. (2024). Short Term Forecasting of Solar Irradiance Using Ensemble CNN-BiLSTM-MLP Model Combined with Error Minimization and CEEMDAN Pre-Processing Technique. Journal of Solar Energy Research, 9(1), 1763-1779. doi: 10.22059/jser.2024.369290.1363

DOI: 10.22059/jser.2024.369290.1363

upcoming years it will be the cheapest source for green energy. However, there is one major downside of solar energy that is its variability in power generation and it depends on seasons and weather. Due to these factors, it is necessary to estimate the power that can be harvest at a particular location, this can be done via solar irradiance forecasting.

In pursuit of enhancing solar irradiance prediction accuracy, various prediction techniques have been proposed and evaluated. These methods include physical models, traditional statistical methods and persistence models. Persistence models are simple, assumes that future solar irradiation will be the same as it is now, so these models are limited to low accuracy as they do not consider variable environmental conditions. These models are helpful to set reference for accuracy in prediction and serves as benchmark for more advance models. Whereas physical models take care of variability of factors that impact the accuracy such as weather conditions, position of sun and many more. In spite of greater accuracy, physical models are usually computationally more expensive. In the reference [1] they examined machine learning models and physical models and found out machine learning models are comparably more beneficial for the forecasting. Traditional statistical approaches for predicting solar irradiance involve time series analysis and statistical modelling techniques to extract patterns and trends from historical data. These approaches include ARIMA, STL, and statistical regression models.

In current scenarios with the advancement of DNNs (deep neural networks), they become the primary elements for ensemble models, such models have proven their supremacy over standalone models specially in the field of solar irradiance forecasting. Spatial and temporal characteristics have been extracted using LSTM-CNN model by the authors and the overall inspection findings demonstrated that ensemble models have greater potential than standalone models across various climatic and atmospheric factors and can be a better choice for immediate forecasting [2]. Despite the fact that combined approaches may employ the different capabilities of multiple models to predict subsequent input patterns based on existing data however, the most relevant data from the raw data cannot be thoroughly extracted by solely relying on ensemble models. As a result, ensemble models frequently pair with signal processing techniques to enhance the model's interference prevention capacity [3]. WPD and EEMD signal processing methods are commonly used in forecasting irradiance. In reference [4] researchers have used EEMD along with deep learning network, and they found out that inclusion of EEMD minimize the effect of variability for long-term prediction hence improves prediction accuracy.

Ke Yan et al. [5] proposed a new technique to detect fault in air handling units using imbalanced data samples. The traditional model face a problem of local minima in which unstable the system and decrease accuracy. The experimental result declare that propsoed model performance is better in all aspects. Hangxia Zhou et al. [6] developed a solar energy forecasting technique with a combination of artificial intelligence technique and internet of things. To remove the photovoltaic energy fluctulations problem, attention mechanism with deep learning model is used with three stages: training, testing and validation. Feng Zhong kai et al. [7] developed a model that combine data decomposition technique with deep learning model and grid search algoruthm is used to optimize the parameters of forecasted model. The propsed model use a relationship between network topology structure to identify the hyperparameters. The evaluation metrics result verify that propsoed model performance is better as compariosn to traditional model. In a study by Saeed Iqbal et al. [8], used a various meterological and environmental factors to investigate the difference between actual and measured temperature value to investigate power loss in the system, same as Mustafa et al. [9] used various environemntal factors have a considerable effect on the output of photovoltaic systems. The major four parameters are used to measure the effeciency of photovoltaic module. To forecast solar irradiance, data-driven methods used by Benali L et al. [10]. The author forecast three components: global horizontal irradiance, direct normal irradiance and direct horizontal irradaince using naïve predictor, artificial neural network and random optimization forest method. The developed model performance are judge using normalized RMSE while L.Cornejo Bueno et al. [11] used a satellite data to forecast solar radiation using artificial intelligencce model. The data of Toledo Spain is used for training and testing.

A machine learning method for solar power forecasting using hyperparameter selection technique. The optimiztion techique select the best parameter for machine learning model in which remove the huge amount of errors and increase accuracy, on the same path, william VanDeventer [12] implement support vector machine with genetic algorithm to predict solar power. The weather paramertes of Deakin University are optimized using genetic algorithm and use as a input of support vector machine model. The RMSE and MAPE are two

metrics used to evaluate the effectiveness of the suggested framework.

Ahzam Shadab et al. [13] develop Autoregressive integerated moving average model with Box-Jenkis approach to predict solar irradiation using thirty four year satellite data of Jamia Millia Islamia University; New Delhi. The time series data is select using acutorcorrelaion function for regression model to forecast solar radiation while Sujan Ghimire et al. [14] utilize various models like as support vector machine, genertic programing model and time and fourier series model for forecast solar radiation. The data of five solar rich cities of Australia are used to check the performance of predictor model. The evaluation process is checked using Legates and McCabe Index value, Mean Absolute percentage Error and Willmott's index calculation error.

Haixiang Zang et al. [15] implement a three different-2 model to predict daily diffuse solar radiation. The five meterological parameters: temperature, humidity, pressure, clear sky index and sunshine ratio used as a input of forecasted model. The twenty year dataset of Lhasa and Urumqi and ten year dataset of Beijing and Wuhan of China are used for training and testing respectively. The photovoltaic power is predicted by Jin Dong et al [16] using uncertain basis function method.The data is taken from 13.50KW photovoltaic panel for trainig and testing. The accuracy of the propsoed model are compared with traditional model to showing the substantial improvement in the energy produced.

Ying Deng et al. [17] implement a ensemble model using error correction strategy to predcit wind speed. The author improve the error correction series to increase the accuracy of hybrid model in which make by a combination of autoregressive integerated moving avergae with variational mode decomposition while Raj Kumar Sahu et al. [18] predict short and medium range solar radiation using Extreme learning Machine model optimized by tecaching learning technique. The forecasting is performed for one hour, one day and one month ahead and performance is measured various evaluation metrics: Mean Absolute Percentage Error, Root Mean Square Error and Correlation Coefficient.

The bidirectional deep learning model is used to forrecast irradiation component by Cong Li et al. [19] The prediction is performed hourly basis and twenty five stations used for checking the performance of developed model in different-2 climate conditions. On the same platform Pardeep singla et al. [20] used double decomposition with bidirectional model. One decomposition is used for decomposong the time series data and second one decomposition is used for preprocessing the error series. The author also use hypothesis test to validate the performance of developed model. The proposed model is tested using Mean Absolute Percentage Error, Root Mean Sqaure Error, Percentage Improvement and Diebold Mariano test. The same author implement twenty four ahead solar forecast using a hybrid model by making a combination of bidirectional long short term memory and wavelet decomposition technique.

Cong Feng et al. [21] used skyimages for irradiance forecasting by implementing deep learning model. The author forecast ten minute to sixty minute ahead forecast using six year data. The forecast score value of deep learning model is better as comparison to smart persistence model.

Samar Fatima et al. [22] implement Monte Carlo Simulation mechanisum to measure the assessment of low voltage distribution system. The proposed method is tested for sub urban area by locating rooftop photovoltaic panel. The method is tested for tow parameters using location and capacity.

The measurement of air quality is the primary concern in today's scenario and for this Zhaohua Wu et al. [23] develop a hybrid Biderectional long short term memory with wavelet transform preprocessing technique ensemble model to predict the quality of air. The measurement of air quality is very dificult due to nonavaliability of historical time series data of air and changing behavior of air qualtiy index. For the evaluation, various parameters are used like as: mean absolute percentsge error, root mean square error and correlation coefficent.

VMD signal processing is used by Rijul Kumar Srivastava et al. [24] along with the predictor for irradiance forecasting and they compared the results with models without signal processing techniques. Their outcome showed that hybrid approach performs better in all perspectives. Prasad et al. [25] weekly irradiance forecasting is accomplished by utilizing dual decomposition approach to broke down the irradiance series into empirical modes. They concluded that MEMD-SVD-RF hybrid model gives more authentic results with greater accuracy. Researchers in reference [26] have taken the advantage of each approach by combining to propose a hybrid model that consist CNN-LSTM neural network and WPD signal processing and by analysing the findings of the research shows proposed approach gives considerable improvement in forecasting accuracy. Tong et al. [27] have proposed a unique approach to forecast irradiance by correcting the error associated with forecasting and they were able to reduce the RMSE approximately by 16.38%.

Table 1. Literature review of the existing study

Author(year) & refference	Input data	Technique used	Result
L.Cornejo-Bueno et al.(2019) [11]	Clear sky, irradiance, CI	ELM	RMSE=60.60W/m^2
A.Shadab et al. (2019) [13]	Sequential solar data	Seasonal ARIMA	MPE= 1.4
J.Dong et al. (2020)[16]	Oak Ridge National Laboratory	Photovotaic data	MAPE=5.72% n-RMSE=7.43%
Ying deng et al. (2020)[17]	Meterological data	EWT+ENN	MAPE=2.35%
Rajkumar Sahu et al. (2021)[18]	Monthly solar radiation data	ELM	MAE=7.53W/m^2, MAPE=14.77%
Cong Li et al. (2021)[19]	Meterological data	BiLSTM	RMSE=22.43W/m^2
Pardeep singla et al. (2022)[20]	Time series data	BiLSTM+FWPD	RMSE=17.55W/m^2, MAPE=2.65%
Cong Feng et al. (2022)[21]	Six year Cloud data	CNN	Forecasting skill improvement from 20 to 39%
Samar Fatima et al. (2023)[22]	Photovoltaic data	Monte carlo Method	Increment of solar photovoltaic generation by 40%
Pardeep Singla et al. (2022)[28]	Time Series data	WT+LSTM	MAPE=1.97%
Zarei et al. (2023)[29]	Grid data	LSTM	20% increment in optimal demand response
Mohit Bhargawa et al. (2023)[30]	Weather conditions	Bamboo cotton wick	Daily productivity of solar increased by 19%
Stocia Dorel et al. (2022) [31]	Wind data	Offgrid PV wind fuel cell system	Design best off grid system with backup facility
Eyup Akpınar et al. (2018) [32]	Photovoltaic data	Snubber technique	Design of high gain boost converter
Li Pan (2023)[33]	24 hour photovoltaic data	ARO algorithm	Maximize the profitibilty of photovoltaic data

Although in the literature authors have used various approaches for forecasting but still some limitations can also be found;

1) The current suggested model's accuracy in forecasting and adaptability for varying local environmental conditions in dealing with variable and intermittent irradiance measurements need to be enhanced further.
2) There have been a few studies on how to use a suitable decomposition approach to include error minimization via stepwise forecasting in order to increase the model's forecasting accuracy.
3) Since the volume of modal decomposition is uncontrollable, aliasing mode and pseudo-mode complications quickly arise, which slightly restrict the model's overall performance.
4) In wavelet transformation, a technique commonly used in conventional research, the method of decomposition is greatly influenced by the experimentally chosen wavelet kernel. The dataset's suitability for the kernel has a direct impact on its forecasting accuracy.

Accordingly, an innovative forecasting architecture of hourly stepwise prediction for solar energy by combining different models such as MLP, Bi-LSTM, CNN, along with error minimization and CEEMDAN decomposition to make a hybrid model (CEEMDAN-CNN-BiLSTM-MLP) was developed to further increase the model's reliability, adaptability, and suppression of interference capability.

Thus, the purpose of this manuscript and its primary contribution are described below.

- **Unification of hybrid model:** The distinctive unpredictable nature of the irradiance series is successfully handled by utilizing the unique

strengths of multiple models. In this article, DBN with a more rapid convergent rate has been utilized for sub-sequence with comparatively high-frequencies forecasting in the 2nd phase of progressive forecasting, along with the CNN-BiLSTM-MLP featuring the advantage of short-term as well as long-term retention.

- **Data partitioning:** CEEMDAN signal pre-processing techniques is implemented to decompose data into various IMFs and also remove mode mixing effect occurred in the traditional approach.
- **Error Minimization:** In this study, the targeted rectification mistakes generated by the step-by-step prediction scheme were used to further increase prediction accuracy.
- **Improvement of predicted results:** The deviation between real values and target values is removed by adjusting the predicted values to get rid of deviation. The divided decomposition series are predicted by different-2 model. High frequency subseries given as an input to deep belief network while low frequency sub series are modelled by CNN-BiLSTM-MLP. The Prediction of different subseries using different model reduced mutual interference and improve comprehensive performance of the model.

2. Proposed Architecture for Forecasting

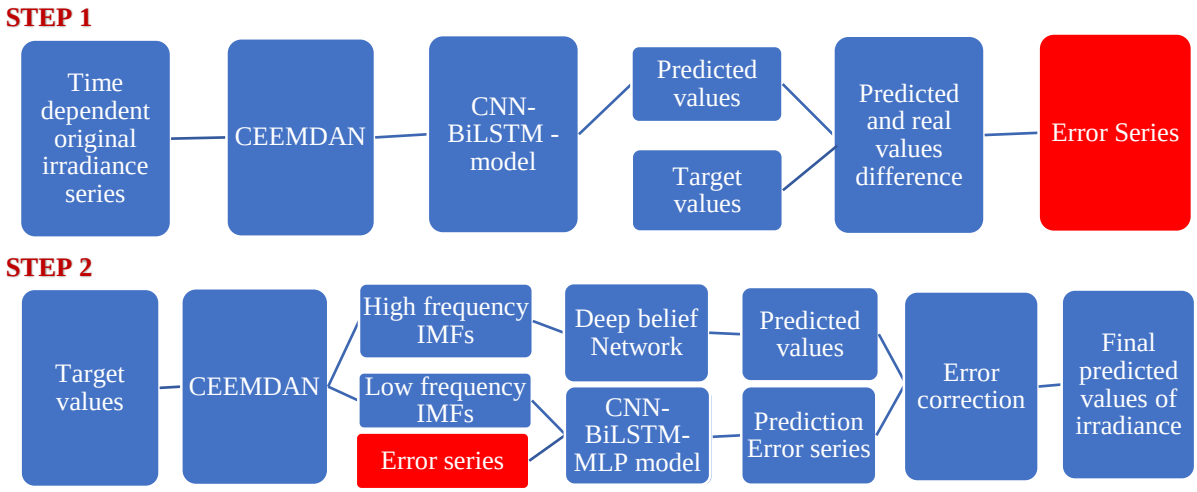

Figure 1: Block Diagram of irradiance forecasting in step-wise manner.

In order to address the irregular, significant fluctuations, and unpredictability associated with solar irradiance, this segment proposes an innovative forecasting system that integrates CEEMDAN, CNN-BiLSTM-MLP and error minimization into a unified composite framework. Solar irradiance forecasting is split into two phases in this system, and the technique fully utilizes the integrated hybrid model's excellent anti-interference capability. Figure 1 displays the proposed framework of the developed system whereas Figure 2 describes the detailed process of proposed architecture from time irradiance series to analysing performance of the model. The brief overview of proposed framework is given below:

- **Error estimation step:** As shown in Step 1 in Figure 1, Time-dependent original solar irradiance series, which mainly incorporates moisture content, GHI, temperature and airspeed are fed to CNN-Bi-LSTM-MLP model and then error is then estimated by comparing model's output to the expected output and hence error series is created.
- **Error removal step:** In step 2, the errors from step 1 are used to alter the final irradiance forecast. Initially, the testing dataset that was separated in the initial step will be the input dataset for the second step; it will be separated into learning and validation datasets into ratios of 40% and 20%. The training and test sets are deconstructed into low-frequency and high-frequency components using the CEEMDAN approach. After that, the impact and distribution of the IMF's intrinsic components are presented. The low-frequency, high-frequency, and errors

are fed to CNN-BiLSTM-MLP and Deep belief network for learning and finishing the forecasting. At last, the corrected solar energy predictions can be obtained by combining the correction errors with the solar energy predictions obtained from the model's output.

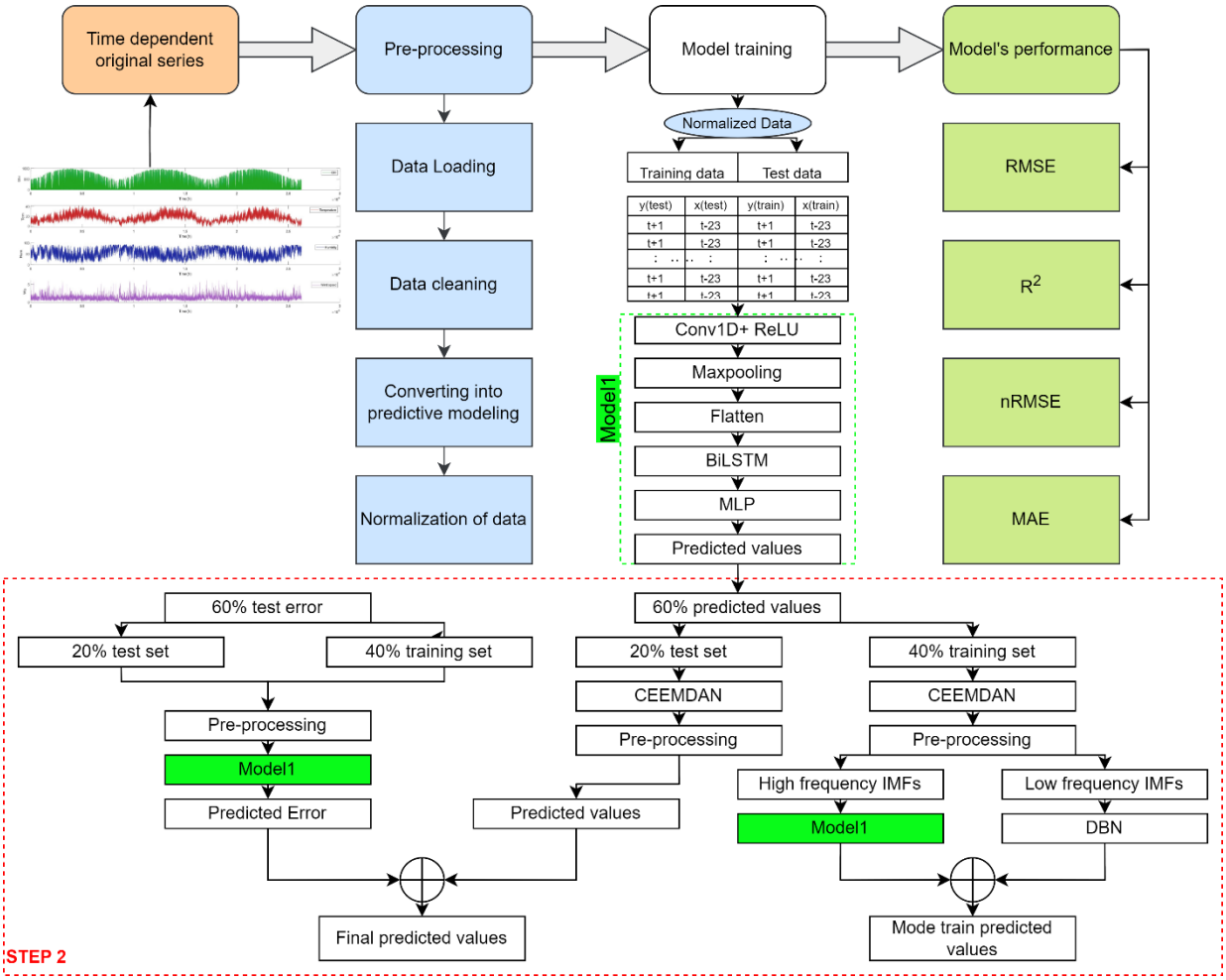

Figure 2. Diagram of proposed structure for forecasting by utilizing integrated ensemble model along with error elemination and CEEMDAN signal processing techiniques.

3. Methodology

3.1. CEEMDAN

As the solar radiation has variabilities, irregularities the data should be refined to efficiently forecast solar irradiance. In this manuscript CEEMDAN is used to break-down the data into periodic modes called (IMFs)intrinsic mode functions, the real data is broken down into fifteen IMFs. It is ideal for analysing the segmenting unpredictable and fluctuating attributes of near-instantaneous radiance. CEEMDAN decomposition outcomes on the time-dependent solar irradiance series are presented in Figure 3. Here is how CEEMDAN works:

1) At first there is addition of noise standard error (φ_0) and Gaussian noise (ω^n) to the real time series (I_s), given by

$$I_s^n = I_s + \varphi_0 * \omega^n;\ n = 1,2 \dots \dots m \quad (1)$$

2) Decomposition of data by EMD is given by equation

$$IMF_1 = \left(\frac{1}{m}\right) * \sum_{k}^{m} \mathrm{IMF}_1^k \quad (2)$$

$$R_1 = \mathrm{I}_s - IMF_1 \quad (3)$$

Where, IMF_1 is first intrinsic mode and R_1 is residual.

3) To obtain other IMFs following equations can be used

$$IMF_{m+1} = \left(\frac{1}{m}\right) * \sum_{k}^{m} \mathrm{EMD}_1 * (R_m + \varphi_1 EMD_1(\omega^n) \quad (4)$$

$$R_m = \mathrm{R}_{m-1} - IMF_m \quad (5)$$

4) At last, the initial signal I_s can be obtained by:

$$O_s = \sum_{k=1}^{S} IMF_{k(s)} + R_s \quad (6)$$

Where, R_s is final residual.

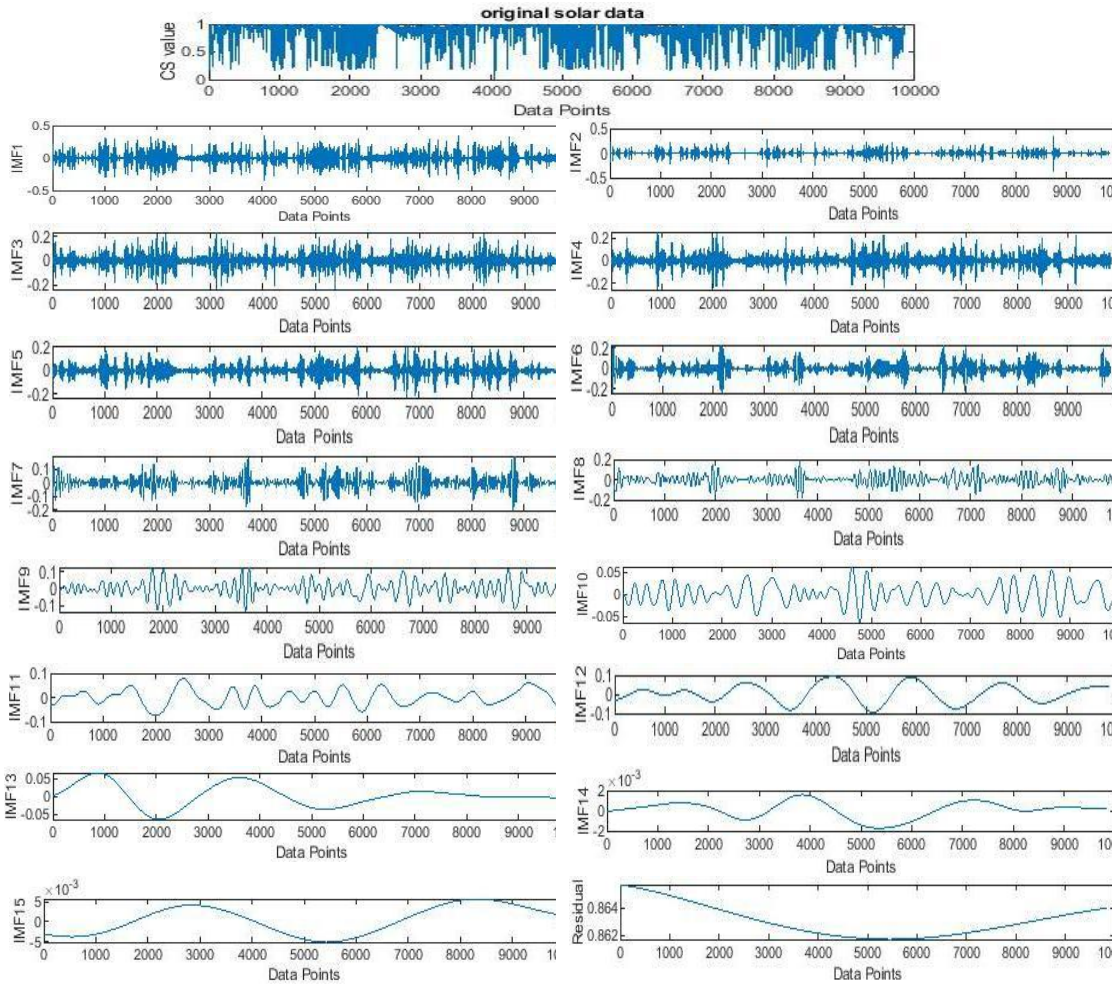

Figure 3. Outcomes of CEEMDAN decomposition.

3.2. CNN

Convolutional Neural Networks (CNNs), a specific kind of neural network, have been developed specifically to handle structured input that resembles a grid. Although, it is proven that CNN is highly successful method for automatic feature extraction in computer vision domain, it is not only limited to this field but it can used where there is time series data such as in solar irradiance forecasting. Feature extraction equation for single dimensional is given by:

$$Y_s = sigmoid\left(\sum_{t=0}^{n-1} W_t * I_{s+t} + b\right) \quad (7)$$

Where, Y_s is output feature, I_{s+t} is input time series, W_t are weights, b is bias and σ is activation function.

3.3. Bi-LSTM

Bi-LSTM contains one forward LSTM and one backward LSTM model which enables Bi-LSTM model to process twice the data that LSTM model can process as shown in Figure 4. It is capable of modelling time series data of solar radiation and associated factors, determining their correlations, and finally producing accurate forecasts. unlike LSTM it not only uses the past data but also depends upon the future values which leads to better learning of model and minimum error between actual and forecasted values. However, the performance of the model depends on the nature of the problem at hand, as well as the quantity and quality of the training data.

$$H_f = sigmoid\left(W_1 * SI_I(t) + W_2 * H_{(f-1)} + a_{H_f}\right) \quad (8)$$

$$H_b = sigmoid\left(W_3 * SI_I(t) + W_5 * H_{(b-1)} + a_{H_b}\right) \quad (9)$$

$$SI_o = W_4 * H_f + w_6 * L + a_{SIO} \quad (10)$$

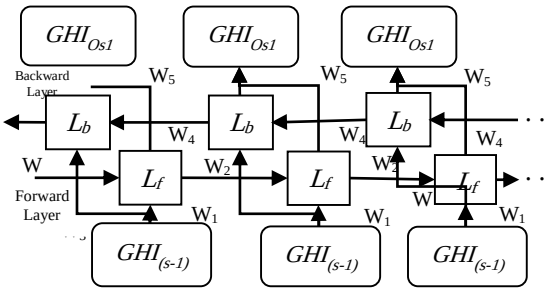

Figure 4. Block diagram of Bi-LSTM approach.

3.4. DBN

It is a widely recognized and efficient neural network approach, comprising multiple layers of interconnected also known as Deep belief network. It is made up of several layers of stochastic, latent variables (hidden layers). The design comprises of a feed stage, many hidden stages, and an output stage, each of which is completely linked to the one above it but not to the levels below it. High frequency sub-sequences in the step-2 are decomposed by CEEMDAN algorithm is accomplished by utilizing a DBN with three hidden layers.

DBN model in terms of Energy function is given by:

$$\varepsilon(v,h) = -\sum_{l} a_l v_l - \sum_{m} b_m v_m - \sum_{l,m} v_l h_m \omega_{l,m} \quad (11)$$

Where, a_l and b_m are bias of the visible and hidden unit, $\omega_{l,m}$ is bias between hidden and visible unit, 'v' and 'h' are visible and hidden unit.

4. Performance Metrics

To evaluate the model's performance that how much deviation is there between Real and Predicted values some evaluation parameters should be used. Here in this manuscript RMSE: Root Man Square Error, MAE: Mean Absolute Error, R^2: determination coefficient and n-RMSE: Normalized Root Mean Square Error are used.

$$RMSE = \sqrt{\frac{1 * \sum_{s=1}^{t}[T_s - P_s]^2}{t}} \quad (12)$$

$$nRMSE = \frac{1}{P_{s_{mean}}}\sqrt{\frac{1 * \sum_{s=1}^{t}[T_s - P_s]^2}{t}} \quad (13)$$

$$MAE = \left(\frac{1}{t}\right) * \sum_{s=1}^{t}[T_s - P_s] \quad (14)$$

$$R^2 = 1 - \frac{\sum_{s=1}^{t}[T_s - P_s]^2}{\sum_{s=1}^{t}[T_s - P_s]} \quad (15)$$

5. Data Description

This manuscript includes time series data of GHI component of solar irradiance of location New Delhi and Ahmadabad; as per the Koppen classification of climate both these locations have mixed climate that have four seasons; summer, monsoon, winter, autumn. Dataset of solar irradiance of these locations is taken from NSRDB (National solar radiation database) for the period of four years; (2009-2014). Apart from the pre-processing of data, deep neural network hyperparameters should also be defined for the better accuracy. To select the optimum values of hyperparameters the data is split into three categories; training, testing and validation. In this research data is split into ratio of 75:25, that is 75% data is used for training and validation and 25% data is used to test the developed model's performance.

Table 2 summarises the necessary information from these collected datasets. Figure 5 depicts a graphical representation of the data.

Table 2. GHI Statical data for both locations.

Location	Summer		Monsoon		Winter		Autumn		Annual	
	Mean	SD	Mean	SD	Mean	SD	Mean	SD	Mean	SD
New Delhi	664.6	220.14	595.39	217.79	389.56	194.73	470.02	189.4	541.13	233.99
Ahmadabad	722.99	200.44	580.8	223.85	502.2	197.8	532.87	195.83	593.95	221.62

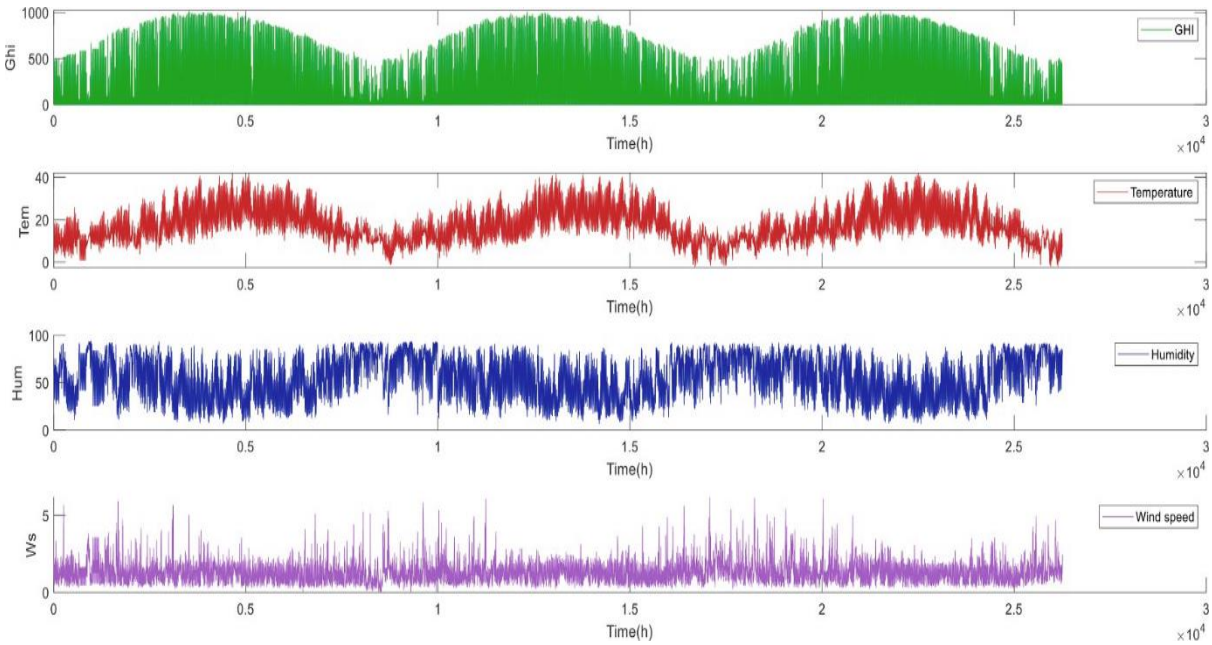

Figure 5. Graphical representation of extracted features of New Delhi data.

5.1. Hyperparameter

There are no rules or restrictions of any kind to choose the hyper-parameter in the literature survey. By altering the parameter values within a specific range, the hyper-parameter may be selected. The grid search approach is used in this research to extract the hyper-parameters for the models from the learning and validation dataset. Table 3 shows the selection of a hyper-parameter within a specific range. Figure 6 depicts the process flow chart of the hyper-parameter selection procedure.

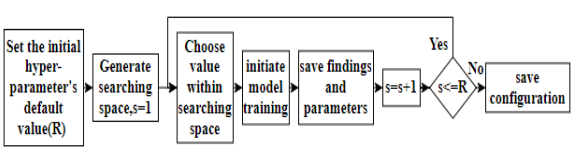

Figure 6. Flow diagram of process of hyper-parameter selection.

The rules for choosing hyperparameters are as follows:

- Set the initial hyperparameter's default value.
- Choose the appropriate activation function.
- Select the ideal batch count and epoch value.
- Choose a suitable optimizer.
- Select the suitable hidden unit value.
- Choose the ideal drop rate.

Table 3. Hyper-parameters

Model	Hyper parameter	Hyper parameter search space	Optimized values
CNN-BiLSTM-MLP	Hidden unit 1	[100-800]	200
	Hidden unit 2	[100-600]	200
	Activation function	[ReLU, Tanh]	ReLU
	Epochs	[50-200]	100
	Optimizer	[Adam, RMSprop]	Adam
	Batch count	[10-12]	12
	Drop rate	[0.1-0.3]	[0.1]

6. Result

This manuscript includes evaluation of the efficacy of hybrid neural network using data from New Delhi and Ahmedabad from 2009-2014, focusing on training and validating a proposed prediction algorithm. In step 2, the following five distinct decomposition techniques were used: WPD, CEEMDAN, CEEMDAN_IMF_6, CEEMDAN_IMF_12, CEEMDAN_IMF_18, EEMD, no decomposition technique (abbreviated as None). Table 4 shows the fundamental parameter values for framework learning after training. Figures 7,8 show the comprehensive and regional forecasted outcomes of both datasets.

Table 4. Essential configurations to train model.

Techniques	Initial inputs	Model (Step-1)	Step 2 inputs	Model (Step-2)		
				Error sequence	Low-frequency	High-frequency
None	$N * 24 * (1 * 5)$	Model-1	Errors, decomposed Intrinsic components	Model-1	Model-1	DBN
EEMD	$N * 24 * (1 * 5)$	Model-1	Errors, decomposed Intrinsic components	Model-1	Model-1	DBN
WPD	$N * 24 * (1 * 5)$	Model-1	Errors, decomposed Intrinsic components	Model-1	Model-1	DBN
CEEMDAN	$N * 24 * (1 * 5)$	Model-1	Errors, decomposed Intrinsic components	Model-1	Model-1	DBN
CEEMDAN _IMF_6	$N * 24 * (1 * 5)$	Model-1	Errors, decomposed Intrinsic components	Model-1	Model-1	DBN
CEEMDAN _IMF_12	$N * 24 * (1 * 5)$	Model-1	Errors, decomposed Intrinsic components	Model-1	Model-1	DBN
CEEMDAN _IMF_18	$N * 24 * (1 * 5)$	Model-1	Errors, decomposed Intrinsic components	Model-1	Model-1	DBN

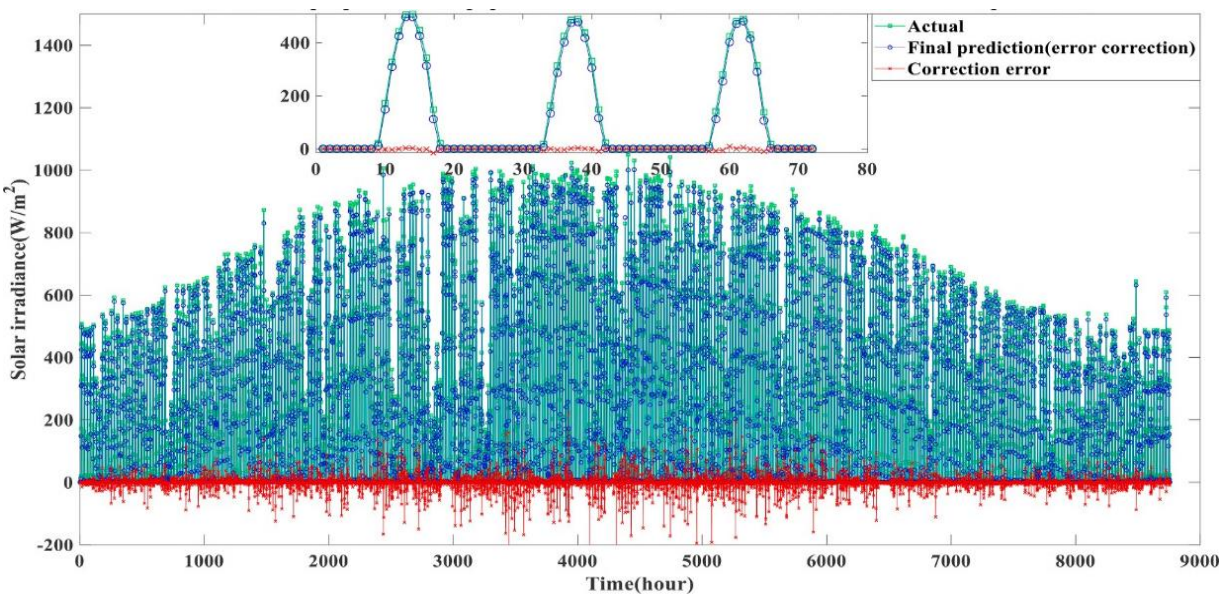

Figure 7. New Delhi forecasting graph.

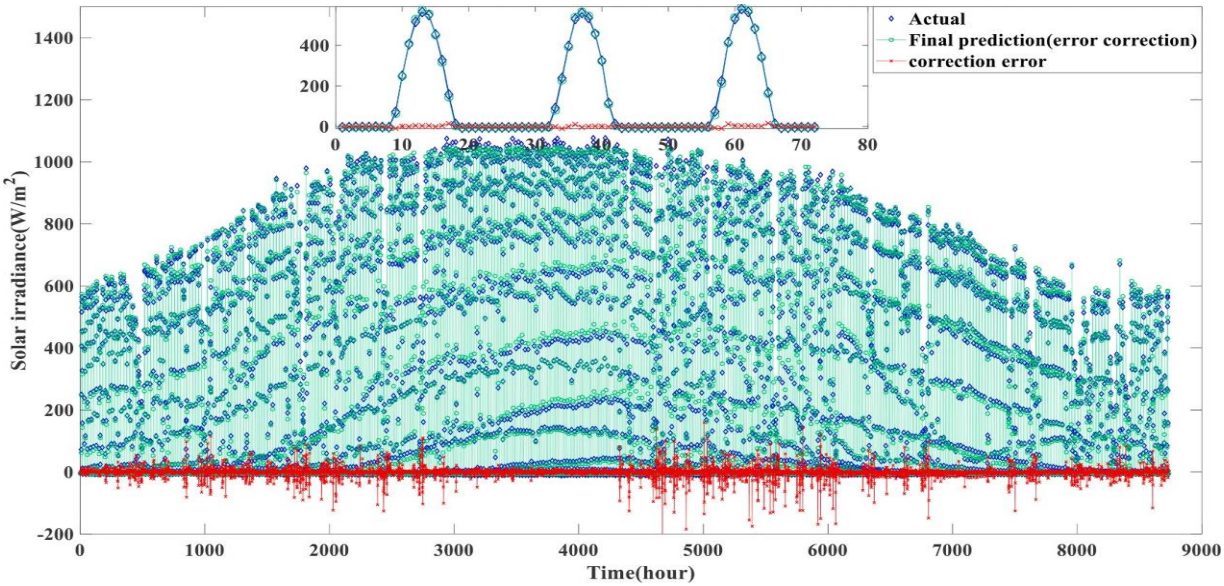

Figure 8. Ahmedabad forecasting graph

Table 5. Final annual performance outcome of both the datasets.

Location		Delhi				Ahmedabad			
Performance matrix		RMSE	n-RMSE	MAE	R^2	RMSE	n-RMSE	MAE	R^2
Method	**Persistence**	102.7	57.42	64.82	81.87	114.6	47.89	71.04	86.56
	None	67.65	33.9	29.86	92.41	45.65	20.15	19.8	96.2
	EEMD	59.96	31.42	33.32	93.58	40.67	18.36	21.34	96.43
	WPD	33.93	16.72	11.97	97.25	28.93	12.85	14.22	99.12
	CEEMDAN	35.41	18.25	18.74	97.16	30.16	18.25	14.99	99.41
	CEEMDAN _IMF_6	38.79	20.04	21.1	96.98	29.54	13.04	16.1	98.98
	CEEMDAN _IMF_12	18.72	10.41	12.46	98.38	14.47	6.16	9.21	99.38
	CEEMDAN _IMF_18	**16.58**	**9.63**	**10.6**	**98.89**	**9.85**	**4.63**	**6.61**	**99.52**

Forecasting on Delhi Data: As depicted in Figure 7, the Delhi data shows the greatest degree of data variability and data volume. Despite the fact that Delhi dataset's outcomes had not been the most favorable among the two data sets, but still the deviation between corrected forecasted values and

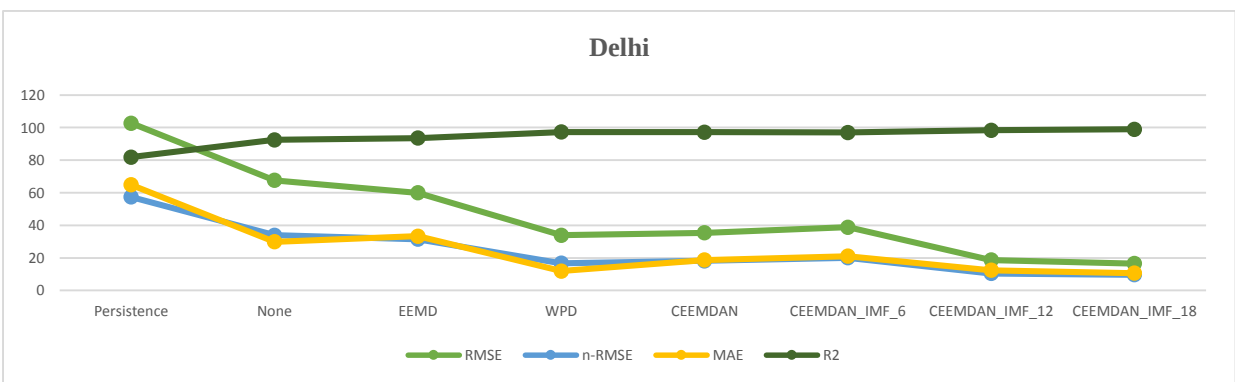

Figure 9. Evaluated performance New Delhi dataset.

target values are minimum as depicted in Figure 7 results is acceptable performance of developed model. In the second step of the analysis, after radiance from sun is broken-down into 18 intrinsic components, from the Table 4 the associated RMSE is 16.58 W/m^2, the normalized RMSE stands at 9.63%, the MAE is 10.6 W/m^2, and the R-squared (R2) value is impressively high at 98.89%, using the proposed forecasting model.

Forecasting on Ahmedabad data: Ahmedabad data shows the least degree of data variability and data volume among both the dataset and is considerably better than Delhi's forecasting as shown in Figure 8. After analyzing the performance of model using Ahmedabad data with 18 sub-series decomposition, it is clear that this dataset gives better outcomes in all perspectives with RMSE equals to 9.85 W/m^2, normalized RMSE is 4.63%, MAE stands at 6.61W/m^2 and the R-squared (R^2) is at 99.52% as mentioned in Table 5.

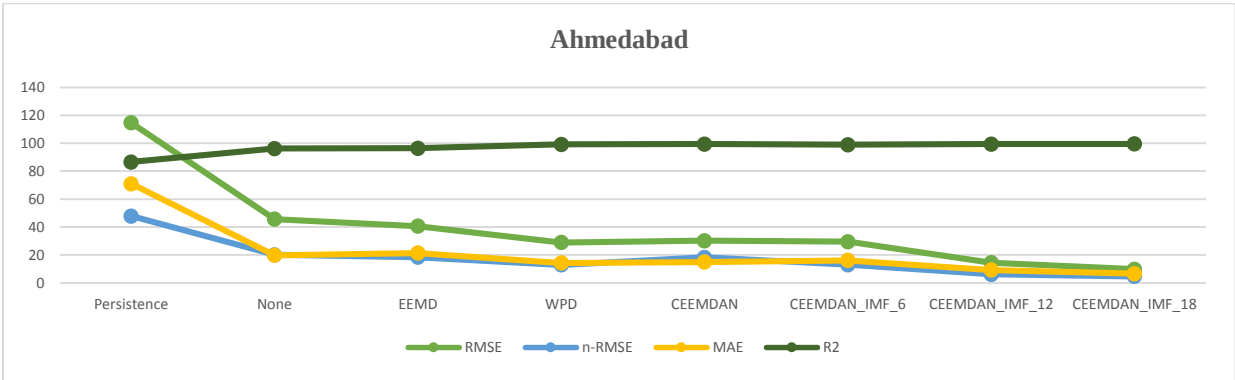

Figure 10. Evaluated performance of Ahmedabad dataset.

7. Comparison analysis of the results

In order to compare the performance of the developed model, persistence model is generally used as benchmark model. In this manuscript, developed model's performance with both the dataset are individually compared with the persistence model along with evaluation of improvement percentage based on Table 5 data and persistence model. Table 8 shows the percentage improvement of the most efficient model over persistence model.

7.1. Analysis of local prediction and influence

To examine the results in more depth, Figure 11 presents a visual representation of the true and predicted Global Horizontal Irradiance for three successive days, spanning from April third to the sixth and September third to the sixth. These two months have been chosen to demonstrate the results due to extreme outcomes as in April RMSE is minimal and maximum in September. For better understanding, these two months are chosen to show the graph of true and predicted GHI of developed model. Figure 11 clearly shows that the significant fluctuations in the true GHI curve resulted in higher inaccuracies in the outcomes. For example, April exhibits a smooth curve because of sunny weather, which the developed framework can effortlessly track. In contrast, the true GHI fluctuates occasionally in September as there are clouds and rains causing highest performance drop as it is difficult to track. This leads to the observation that there is a decline in resemblance between the true and forecasted GHI as fluctuations increase in true GHI; vice versa, resemblance will improve when fluctuations decrease. However, the developed framework also accounts for the ambiguities present in the true GHI within tolerable variations. Consequently, such findings suggest the proposed framework is an effective prediction tool for all climates.

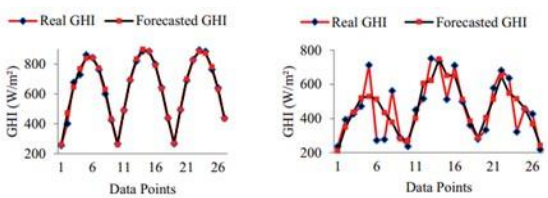

Figure 11. Performance of developed approach.

7.2. Evaluation of various seasons performance and study of prediction error

To advance the models annual prediction performance by strengthening the model's complete ability to predict outcomes in subsequent investigations. In this study, forecasting impacts of two datasets with different seasonal conditions are examined in-depth individually. Below is a description in more detail.

7.3. The Delhi dataset's performance evaluation findings for various seasons are as follows:

The associated outcome evaluation indicators have been measured separately using several predictions approaches due to the Delhi dataset's relatively significant variability. Based on the estimated results, it is clear that the data set possesses comparatively higher level of fluctuations in fall and summertime, and a lower level of fluctuation in the winters and springtime when the solar irradiance data are not decomposed. The performance metrics calculated using the prediction approach presented in this research are the best-case scenarios. In Table 6 the outcome evaluations for different seasons are displayed.

Table 6. Seasonal performance of New Delhi data using different signal processing techniques.

Seasons	Performance matrix	Method						
		None	EEMD	WPD	CEEMDAN	CEEMDAN _IMF_6	CEEMDAN _IMF_12	CEEMDAN _IMF_18
Spring	RMSE	52.17	53.67	26.48	22.31	29.38	16.49	**15.21**
	n-RMSE	34.70	35.12	17.21	14.41	19.08	11.20	**9.71**
	MAE	22.45	28.05	8.54	11.90	16.06	10.68	**9.26**
	R^2	93.12	93.09	97.49	97.93	97.18	98.34	**98.43**
Summer	RMSE	89.10	74.64	41.69	48.58	48.21	22.02	**18.65**
	n-RMSE	33.78	29.11	16.00	19.84	19.18	8.16	**7.82**
	MAE	39.78	43.55	14.43	24.74	25.95	14.14	**11.81**
	R^2	91.14	93.47	97.21	96.60	96.75	98.49	**98.32**
Autumn	RMSE	88.21	65.41	47.45	48.54	49.28	21.89	**18.49**
	n-RMSE	36.15	26.68	19.21	21.24	21.56	9.54	**8.14**
	MAE	39.91	36.59	17.43	25.87	27.54	15.06	**11.89**
	R^2	90.63	94.12	96.41	96.45	96.35	98.31	**99.34**
Winter	RMSE	41.14	46.12	20.11	22.21	28.31	14.50	**13.98**
	n-RMSE	31.00	34.78	14.49	17.52	20.37	12.77	**12.87**
	MAE	17.31	25.12	7.51	12.48	14.86	9.96	**9.45**
	R^2	94.75	93.64	97.89	97.67	97.67	98.40	**99.49**
Annual	RMSE	67.65	59.96	33.93	35.41	38.79	18.72	**16.58**
	n-RMSE	33.90	31.42	16.72	18.25	20.04	10.41	**9.63**
	MAE	29.86	33.32	11.97	18.74	21.10	12.46	**10.60**
	R^2	92.41	93.58	97.25	97.16	96.98	98.38	**98.89**

7.4. The findings of the Ahmadabad dataset performance evaluation in several seasons are as follows:

The associated outcome evaluation indicators have been measured for Ahmadabad data which has less variation than the Delhi data. Based on the calculated results, it is simple to see that the dataset's volatility is mainly indicated in fall season and comparatively have more forecasting error and winters and spring season have comparatively low fluctuations. Table 7 display the various seasonal performance evaluation indicators that were computed.

Table 7. Seasonal performance of Ahmadabad data using different signal processing techniques.

Seasons	Performance matrix	Method						
		None	EEMD	WPD	CEEMDAN	CEEMDAN _IMF_6	CEEMDAN _IMF_12	CEEMDAN _IMF_18
Spring	RMSE	42.17	52.67	26.48	27.31	29.38	13.49	**7.21**
	n-RMSE	22.70	27.12	14.21	14.41	15.08	6.20	**3.71**
	MAE	19.45	28.05	13.54	14.90	16.06	8.68	**4.31**
	R^2	95.12	96.52	98.98	98.93	98.18	99.34	**99.43**
Summer	RMSE	32.10	24.64	25.69	25.58	24.21	15.02	**9.65**
	n-RMSE	9.78	6.86	7.48	7.84	7.18	4.16	**3.82**
	MAE	13.78	13.62	14.41	15.74	13.96	10.14	**7.81**
	R^2	98.14	93.47	99.21	99.60	99.75	99.49	**99.82**
Autumn	RMSE	72.21	53.25	40.45	48.54	39.28	16.89	**13.59**
	n-RMSE	25.15	16.68	14.21	38.24	13.56	5.54	**5.14**

	MAE	30.91	28.59	17.43	19.87	20.54	10.06	**8.89**
	R^2	93.63	98.12	99.41	99.45	99.35	99.31	**99.34**
Winter	RMSE	36.14	32.12	23.11	19.21	25.31	12.50	**8.98**
	n-RMSE	23.00	22.78	15.49	12.52	16.37	8.77	**5.87**
	MAE	15.08	15.12	11.51	09.48	13.86	7.96	**5.45**
	R^2	97.91	97.64	98.89	99.67	98.67	99.40	**99.49**
Annual	RMSE	45.65	40.67	28.93	30.16	29.54	14.47	**9.85**
	n-RMSE	20.15	18.36	12.85	18.25	13.04	6.16	**4.63**
	MAE	19.80	21.34	14.22	14.99	16.10	9.21	**6.61**
	R^2	96.2	96.43	99.12	99.41	98.98	99.38	**99.52**

7.5. Percentage Improvement

Percentage improvement is one more criterion used to determine a superior model from other options and Table 8 shows the performance improvement of different models to the persistence model. Percentage improvement can be calculated as:

$$P_i = \frac{|i_{per} - i_m|}{i_{per}} \quad (16)$$

Where, 'i' is the metrics used such as R^2, $RMSE$, $nRMSE\ and\ MAE$ and 'm' represents different models used and 'per' is persistence model.

Table 8. Performance improvement of different models compared to persistence model.

Percentage improvement	Dataset	None	EEMD	WPD	CEEMDAN	CEEMDAN _IMF_6	CEEMDAN _IMF_12	CEEMDAN _IMF_18
P_{RMSE}	Delhi	34.12	41.61%	66.96%	65.52%	62.22%	81.77%	**83.85%**
	Ahmedabad	60%	64.51%	74.75%	73.68%	74.22%	87.37%	**91.4%**
P_{nRMSE}	Delhi	40.96%	45.28%	70.88%	68.21%	64.99%	81.87%	**83.22%**
	Ahmedabad	57.92%	61.66%	73.16%	61.18%	72.77%	87.13%	**90.33%**
P_{MAE}	Delhi	53.93%	48.59%	81.53%	71.08%	67.44%	80.77%	**83.64%**
	Ahmedabad	72.12%	69.96%	79.98%	78.89%	77.34%	87.04%	**90.69%**
P_{R^2}	Delhi	12.87%	14.3%	18.78%	18.67%	18.45%	20.17%	**20.78%**
	Ahmedabad	11.14%	11.4%	14.51%	14.84%	14.34%	14.81%	**14.97%**

8. Comparison existing models

Moreover, to assess the effectiveness of the strategy suggested in this work more thoroughly and objectively. With the plan of this work, some systems that have been offered in recent years are likewise validated. **Error! Reference source not found.** provides a more intuitive illustration of it. In comparison to some research that have been reported in the literature, the proposed model yields encouraging results.

Table 9. Existing model comparisons.

Author and year of publication	Models	Region	Time horizon	RMSE(W/ m^2)	MAPE (%)
Zang et al,2020 [15]	CNN and LSTM	Texas, USA	1-hr	69.26	-
Li et al, 2021 [19]	BiLSTM	United State	1-hr	98.44	-
Singla., et al, 2021 [28]	WT-BiLSTM	Ahmadabad	24-hr	45.61	6.48
Gupta, A., et al 2022 [34]	EEMD-GA-LSTM	New Delhi	1-hr	-	3.23
Gupta, A., et al 2022 [35]	CEEMDAN, GA and BiLSTM	New Delhi	1-hr	-	2.23
This Work	**CEEMDAN-CNN-BiLSTM-MLP (Proposed Model)**	**New Delhi, Ahmedabad**	**1-hr**	**13.215**	**1.878**

9. Conclusion

This work proposes a hybrid forecasting model that addresses the issue of poor reliability and adaptability of forecasting methods used for solar energy forecasting. It uses the integrated ensemble model CNN-BiLSTM-MLP along with error minimization and CEEMDAN for forecasting solar energy for the next hour. In this research, the CEEMDAN technique is employed in the second phase of the prediction process to break down the irradiance dataset. Furthermore, only time series data were taken into consideration in the study; structured datasets may potentially be integrated with time series data to improve performance. This approach effectively tackles the challenge posed by the considerable noise and variability in solar irradiance data. Traditional preprocessing techniques struggles with managing several decomposition modes in such noisy data, leading to issues like aliasing when under-resolution misleading clusters when over-resolution. By evaluating thoroughly, the proposed framework showed better reliability and accuracy in comparison to currently developed approaches when evaluated using datasets from Delhi and Ahmedabad. The ideal prediction system (in this case CEEMDAN_IFM_18) reduces RMSE, n-RMSE, and MAE by 13.215 W/m^2, 7.13%, and 8.605 W/m^2, respectively on average, and increases R^2 by 17.875% when compared to the persistent model.

Beside the fact that this model outperforms other currently developed models for next hour forecasting but because of the challenging nature of climate variations in winters and monsoon, this proposed framework predicts irradiance based on previous irradiance data and can struggle tackle sudden variations effectively. Future work will include more parameters such as visibility, live climate data which will further improve the accuracy and adaptability and will be able to do long hour forecasting.

Nomenclature

GHI	Global horizontal irradiance
I_s	Real time series
φ_0	Standard error
ω^n	Gaussian noise
IMF_1	First intrinsic mode
R_1	Residual
R_s	Final residual
SI_I	Input layer
H_f	Forward hidden laver
H_b	Backward hidden layer
SI_o	Output layer
$\varepsilon(v,h)$	Energy function
RMSE	Root-mean square error
n-RMSE	Normalized root-mean square error
MAE	Mean absolute error
R^2	Determination coefficient
SD	Standard deviation
P_i	Percentage improvement

References

[1] R. A. A. Ramadhan, Y. R. J. Heatubun, S. F. Tan, and H.-J. Lee, "Comparison of physical and machine learning models for estimating solar irradiance and photovoltaic power," *Renew Energy*, vol. 178, pp. 1006–1019, Nov. 2021, doi: 10.1016/j.renene.2021.06.079.

[2] P. Kumari and D. Toshniwal, "Long short term memory–convolutional neural network based deep hybrid approach for solar irradiance forecasting," *Appl Energy*, vol. 295, p. 117061, Aug. 2021, doi: 10.1016/j.apenergy.2021.117061.

[3] Z. Ma *et al.*, "Application of hybrid model based on double decomposition, error correction and deep learning in short-term wind speed prediction," *Energy Convers Manag*, vol. 205, p. 112345, Feb. 2020, doi: 10.1016/j.enconman.2019.112345.

[4] W. Wang, K. Chau, L. Qiu, and Y. Chen, "Improving forecasting accuracy of medium and long-term runoff using artificial neural network based on EEMD decomposition," *Environ Res*, vol. 139, pp. 46–54, May 2015, doi: 10.1016/j.envres.2015.02.002.

[5] K. Yan, J. Huang, W. Shen, and Z. Ji, "Unsupervised learning for fault detection and diagnosis of air handling units," *Energy Build*, vol. 210, p. 109689, Mar. 2020, doi: 10.1016/j.enbuild.2019.109689.

[6] H. Zhou, Q. Liu, K. Yan, and Y. Du, "Deep Learning Enhanced Solar Energy Forecasting with AI-Driven IoT," *Wirel Commun Mob Comput*, vol. 2021, pp. 1–11, Jun. 2021, doi: 10.1155/2021/9249387.

[7] Z. Feng, W. Niu, X. Wan, B. Xu, F. Zhu, and J. Chen, "Hydrological time series forecasting via

signal decomposition and twin support vector machine using cooperation search algorithm for parameter identification," *J Hydrol (Amst)*, vol. 612, p. 128213, Sep. 2022, doi: 10.1016/j.jhydrol.2022.128213.
[8] S. Iqbal, S. N. Khan, M. Sajid, J. Khan, Y. Ayaz, and A. Waqas, "Impact and performance efficiency analysis of grid-tied solar photovoltaic system based on installation site environmental factors," *Energy & Environment*, vol. 34, no. 7, pp. 2343–2363, Nov. 2023, doi: 10.1177/0958305X221106618.
[9] R. J. Mustafa, M. R. Gomaa, M. Al-Dhaifallah, and H. Rezk, "Environmental Impacts on the Performance of Solar Photovoltaic Systems," *Sustainability*, vol. 12, no. 2, p. 608, Jan. 2020, doi: 10.3390/su12020608.
[10] P. Gupta and R. Singh, "PV power forecasting based on data-driven models: a review," *International Journal of Sustainable Engineering*, vol. 14, no. 6, pp. 1733–1755, Nov. 2021, doi: 10.1080/19397038.2021.1986590.
[11] S. Salcedo-Sanz, R. C. Deo, L. Cornejo-Bueno, C. Camacho-Gómez, and S. Ghimire, "An efficient neuro-evolutionary hybrid modelling mechanism for the estimation of daily global solar radiation in the Sunshine State of Australia," *Appl Energy*, vol. 209, pp. 79–94, Jan. 2018, doi: 10.1016/j.apenergy.2017.10.076.
[12] W. VanDeventer *et al.*, "Short-term PV power forecasting using hybrid GASVM technique," *Renew Energy*, vol. 140, pp. 367–379, Sep. 2019, doi: 10.1016/j.renene.2019.02.087.
[13] A. Shadab, S. Ahmad, and S. Said, "Spatial forecasting of solar radiation using ARIMA model," *Remote Sens Appl*, vol. 20, p. 100427, Nov. 2020, doi: 10.1016/j.rsase.2020.100427.
[14] "Predictive Modelling of Global Solar Radiation with Artificial Intelligence Approaches using MODIS Satellites and Atmospheric Reanalysis Data for Australia."
[15] H. Zang *et al.*, "Estimation and validation of daily global solar radiation by day of the year-based models for different climates in China," *Renew Energy*, vol. 135, pp. 984–1003, May 2019, doi: 10.1016/j.renene.2018.12.065.
[16] J. Dong, T. Kuruganti, and S. M. Djouadi, "Very short-term photovoltaic power forecasting using uncertain basis function," in *2017 51st Annual Conference on Information Sciences and Systems (CISS)*, IEEE, Mar. 2017, pp. 1–6. doi: 10.1109/CISS.2017.7926158.
[17] Y. Deng, B. Wang, and Z. Lu, "A hybrid model based on data preprocessing strategy and error correction system for wind speed forecasting," *Energy Convers Manag*, vol. 212, p. 112779, May 2020, doi: 10.1016/J.ENCONMAN.2020.112779.
[18] R. K. Sahu, B. Shaw, J. R. Nayak, and Shashikant, "Short/medium term solar power forecasting of Chhattisgarh state of India using modified TLBO optimized ELM," *Engineering Science and Technology, an International Journal*, vol. 24, no. 5, pp. 1180–1200, Oct. 2021, doi: 10.1016/J.JESTCH.2021.02.016.
[19] C. Li, Y. Zhang, G. Zhao, and Y. Ren, "Hourly solar irradiance prediction using deep BiLSTM network," *Earth Sci Inform*, vol. 14, no. 1, pp. 299–309, Mar. 2021, doi: 10.1007/s12145-020-00511-3.
[20] P. Singla, M. Duhan, and S. Saroha, "An integrated framework of robust local mean decomposition and bidirectional long short-term memory to forecast solar irradiance," *Int J Green Energy*, vol. 20, no. 10, pp. 1073–1085, Aug. 2023, doi: 10.1080/15435075.2022.2143272.
[21] C. Feng, J. Zhang, W. Zhang, and B.-M. Hodge, "Convolutional neural networks for intra-hour solar forecasting based on sky image sequences," *Appl Energy*, vol. 310, p. 118438, Mar. 2022, doi: 10.1016/j.apenergy.2021.118438.
[22] S. Fatima, V. Püvi, M. Pourakbari- Kasmaei, and M. Lehtonen, "Photovoltaic hosting capacity improvement based on the economic comparison between curtailment and network upgrade," *IET Generation, Transmission & Distribution*, vol. 17, no. 17, pp. 3848–3860, Sep. 2023, doi: 10.1049/gtd2.12936.
[23] Z. WU and N. E. HUANG, "ENSEMBLE EMPIRICAL MODE DECOMPOSITION: A NOISE-ASSISTED DATA ANALYSIS METHOD," *Adv Adapt Data Anal*, vol. 01, no. 01, pp. 1–41, Jan. 2009, doi: 10.1142/S1793536909000047.
[24] R. Kumar Srivastava and A. Gupta, "Short term solar irradiation forecasting using Deep neural network with decomposition methods and optimized by grid search algorithm," *E3S Web of Conferences*, vol. 405, p. 02011, Jul. 2023, doi: 10.1051/e3sconf/202340502011.
[25] R. Prasad, M. Ali, Y. Xiang, and H. Khan, "A double decomposition-based modelling approach to forecast weekly solar radiation," *Renew Energy*, vol. 152, pp. 9–22, Jun. 2020, doi: 10.1016/j.renene.2020.01.005.
[26] X. Huang *et al.*, "Hybrid deep neural model for hourly solar irradiance forecasting," *Renew Energy*, vol. 171, pp. 1041–1060, Jun. 2021, doi: 10.1016/j.renene.2021.02.161.
[27] J. Tong, L. Xie, S. Fang, W. Yang, and K. Zhang, "Hourly solar irradiance forecasting based on encoder–decoder model using series decomposition

and dynamic error compensation," *Energy Convers Manag*, vol. 270, p. 116049, Oct. 2022, doi: 10.1016/j.enconman.2022.116049.

[28] P. Singla, M. Duhan, and S. Saroha, "An ensemble method to forecast 24-h ahead solar irradiance using wavelet decomposition and BiLSTM deep learning network," *Earth Sci Inform*, vol. 15, no. 1, pp. 291–306, Mar. 2022, doi: 10.1007/s12145-021-00723-1.

[29] A. Zarei and N. Ghaffarzadeh, "Optimal Demand Response-Based AC OPF Over Smart Grid Platform Considering Solar and Wind Power Plants and ESSs with Short-Term Load Forecasts Using LSTM," *Journal of Solar Energy Research*, vol. 8, no. 2, pp. 1367–1379, Apr. 2023, doi: 10.22059/JSER.2023.352567.1271.

[30] M. Bhargva, M. Sharma, A. Yadav, N. K. Batra, and R. K. Behl, "Productivity Augmentation of a Solar Still with Rectangular Fins and Bamboo Cotton Wick," *Journal of Solar Energy Research*, vol. 8, no. 2, pp. 1410–1416, Apr. 2023, doi: 10.22059/jser.2023.356414.1279.

[31] S. Dorel, M. Gmal Osman, C.-V. Strejoiu, and G. Lazaroiu, "Exploring Optimal Charging Strategies for Off-Grid Solar Photovoltaic Systems: A Comparative Study on Battery Storage Techniques," *Batteries*, vol. 9, no. 9, p. 470, Sep. 2023, doi: 10.3390/batteries9090470.

[32] E. Akpinar, A. Balikci, E. Durbaba, and B. T. Azizoglu, "Single-Phase Transformerless Photovoltaic Inverter With Suppressing Resonance in Improved H6," *IEEE Trans Power Electron*, vol. 34, no. 9, pp. 8304–8316, Sep. 2019, doi: 10.1109/TPEL.2018.2886054.

[33] L. Pan, X. Xu, J. Liu, and W. Hu, "Adaptive robust scheduling of a hydro/photovoltaic/pumped-storage hybrid system in day-ahead electricity and hydrogen markets," *Sustain Cities Soc*, vol. 95, p. 104571, Aug. 2023, doi: 10.1016/j.scs.2023.104571.

[34] A. Gupta and K. Gupta, "Short Term Solar Irradiation Prediction Framework Based on EEMD-GA-LSTM Method," *Strategic Planning for Energy and the Environment*, pp. 255–280, Feb. 2023, doi: 10.13052/spee1048-5236.4132.

[35] A. Gupta, K. Gupta, and sumit Saroha, "Short Term Solar Irradiation Forecasting using CEEMDAN Decomposition Based BiLSTM Model Optimized by Genetic Algorithm Approach.," *International Journal of Renewable Energy Development* , vol. 11, no. 3, 2022.